AJNR

The "Presyrinx" State: A Reversible Myelopathic Condition That May Precede Syringomyelia

Nancy J. Fischbein, William P. Dillon, Charles Cobbs and Philip R. Weinstein

AJNR Am J Neuroradiol 1999, 20 (1) 7-20
http://www.ajnr.org/content/20/1/7

AJNR Am J Neuroradiol 20:7–20, January 1999

The "Presyrinx" State: A Reversible Myelopathic Condition That May Precede Syringomyelia

Nancy J. Fischbein, William P. Dillon, Charles Cobbs, and Philip R. Weinstein

BACKGROUND AND PURPOSE: **Alteration of CSF flow has been proposed to be an important mechanism leading to the development of syringomyelia. We hypothesize that a "presyrinx" condition attributable to a potentially reversible alteration in normal CSF flow exists and that its appearance may be caused by variations in the competence of the central canal of the spinal cord.**

METHODS: **Five patients with clinical evidence of myelopathy, no history of spinal cord trauma, enlargement of the cervical spinal cord with T1 and T2 prolongation but no cavitation, evidence of altered or obstructed CSF flow, and no evidence of intramedullary tumor or a spinal vascular event underwent MR imaging before and after intervention that alleviated obstruction to CSF flow.**

RESULTS: **Preoperatively, all patients had enlarged spinal cords and parenchymal T1 and T2 prolongation without cavitation. Results of MR examinations after intervention showed resolution of cord enlargement and normalization or improvement of cord signal abnormalities. In one patient with severe arachnoid adhesions who initially improved after decompression, late evolution into syringomyelia occurred in association with continued CSF obstruction.**

CONCLUSION: **Nontraumatic obstruction of the CSF pathways in the spine may result in spinal cord parenchymal T2 prolongation that is reversible after restoration of patency of CSF pathways. We refer to this MR appearance as the "presyrinx" state and stress the importance of timely intervention to limit progression to syringomyelia.**

Syringomyelia occurs in a number of clinical settings, most commonly after trauma (1–3) or in association with a Chiari malformation (4–7). Other causes include infectious or inflammatory arachnoiditis (7–11), tumors of the spine and spinal cord (7), posterior fossa tumors (12), and cervical spondylosis (13). Syrinxes typically appear as well-defined discrete cavities containing fluid that is isointense with CSF on all sequences (14, 15). The pathophysiology of syringomyelia is controversial, but experimental models (16–18) and clinical studies (19) have implicated alterations in CSF flow as a significant factor in the development and progression of certain types of syringomyelia. The hypothesis that CSF normally flows along perivascular spaces within the parenchyma of the spinal cord to the central canal is supported by experimental studies (20–25). Variations in patency of the central canal of the spinal cord have been associated with the development of different types of syringomyelia (18, 26) and most likely play a role in determining the location of a syrinx remote from a focus of CSF obstruction, such as is commonly seen in the Chiari I malformation. The reversibility of syringomyelia after restoration of CSF pathways has been well documented in patients undergoing posterior fossa decompression for Chiari malformations, removal of extradural masses, and lysis of adhesions (9, 12, 27).

We have identified five myelopathic patients with no history of spine trauma who had underlying conditions associated with alterations of CSF flow. These patients had enlargement and T2 prolongation of the spinal cord, without frank cavitation, on MR imaging studies that improved or reversed after restoration of CSF flow pathways. We hypothesized on the basis of historical, imaging, and surgical findings that obstruction to normal CSF flow pathways resulted in the cord enlargement and MR signal abnormalities that reversed after restoration of normal CSF pathways. We also hypothesized that variation in patency of the central canal of the spinal cord plays a role in the genesis of this ''presyrinx'' state.

Methods

Over a 2-year period, five patients who met the following criteria were identified prospectively: clinical evidence of my-

Received March 10, 1998; accepted after revision August 26.

From the Departments of Radiology (N.J.F., W.P.D.) and Neurosurgery (C.C., P.R.W.), University of California, San Francisco.

Address reprint requests to Nancy J. Fischbein, MD, Department of Radiology, Box 0628, University of California, San Francisco, 505 Parnassus Ave, San Francisco, CA 94143.

Summary of Patient Data

Patient	Figure No.	Age (y)/Sex	History	Clinical Condition Pre-op	Previous Surgery
1	1	2/M	Chiari I malformation	Severe headaches, progressive clumsiness in limb movements over the course of 1 y	Limited decompression (suboccipital craniectomy) for Chiari I malformation
2	2	69/F	Polymyalgia rheumatica, previous epidural abscess associated with osteomyelitis of the cervical spine	Progressive quadriparesis, progressive loss of sensation and motor control in hands	Decompression of epidural abscess via C6 laminectomy 18 mo earlier
3	4	41/M	Remote h/o head trauma; basilar arachnoid adhesions; h/o hydrocephalus	Progressive neck pain and spastic quadriparesis	Posterior fossa decompression VP shunt for hydrocephalus
4	3	40/F	Grade III SAH caused by aneurysm, s/p GDC coil embolization; course c/b *S. epidermidis* meningitis	Neck pain and quadriparesis	Coil embolization of aneurysm, external ventricular drainage of CSF
5	NS	77/F	Severe cervical spondylostenosis and mild basilar impression	Progressive weakness in both arms, R > L, and hand numbness; spasticity and incoordination of legs; no neck pain	None

Note.—FM indicates foramen magnum; SAH, subarachnoid hemorrhage; NS, not shown; VP, ventriculoperitoneal; *S. epidermidis, Staphylococcus epidermidis*; h/o, history of; pre-op, preoperatively; post-op, postoperatively.

elopathy, no history of spinal cord trauma, enlargement of the cervical cord with parenchymal T1 and T2 prolongation but no frank cavitation, and no evidence of intramedullary tumor or a spinal vascular event as the cause of cord signal changes. No patient had evidence of active inflammatory or demyelinating disease or received steroid therapy. In addition, all patients had obstruction to CSF flow at the level of the foramen magnum or the spinal epidural or subarachnoid space as evidenced by historical and/or imaging findings. Our patients included two males and three females and ranged in age from 2 to 77 years. Clinical records and imaging studies for these patients were reviewed.

All patients underwent preoperative imaging on a 1.5-T MR system. Imaging sequences included conventional spin-echo T1-weighted images (500/14 [TR/TE], 4 mm thick, 256 × 256 matrix) and fast spin-echo T2-weighted images ($3000/105_{eff}$, echo train length of 8, 3 mm thick, 256 × 256 matrix) obtained in the sagittal plane in addition to axial T1-weighted images. A proton density–weighted sequence was not obtained, since it is not part of our routine spine imaging protocol. Contrast-enhanced images were obtained in three patients and included sagittal and axial T1-weighted sequences. MR examinations were conducted on all patients after surgical intervention and included, at a minimum, sagittal T1-weighted and fast spin-echo T2-weighted sequences. In addition, one patient underwent CT myelography preoperatively, and one patient underwent CT myelography postoperatively. Only one patient had an MR flow study performed preoperatively, using a cine phase-contrast technique (24/minimum [TR/TE], flip angle of 30°, 256 × 128 matrix, flow compensation and peripheral gating applied, velocity-encoding gradient = 5 cm/s) to evaluate CSF flow at the foramen magnum.

Results

A summary of our patients' histories, as well as clinical and imaging findings, is presented in the Table. All patients underwent MR imaging of the cervical spinal cord to evaluate myelopathic symptoms, although in one case (patient 1) headaches were the dominant clinical feature. The clinical presentations were similar to that of patients with central cystic myelopathy (7, 28), including increasing loss of motor function or weakness in all patients, sensory changes in two patients, increased spasticity in two patients, and radicular pain in one patient. The conditions that predisposed our patients to alterations in CSF flow dynamics and myelopathy included the following: Chiari I malformation with severe tonsillar herniation; previous osteomyelitis complicated by epidural abscess, meningitis, and arachnoiditis; basilar arachnoid adhesions related to previous head trauma, traumatic subarachnoid hemorrhage, and posterior fossa surgery; subarachnoid hemorrhage complicated by meningitis, leading to severe hydrocephalus and tonsillar herniation; and rheumatoid arthritis with severe cervical spondylosis and spinal stenosis accompanied by basilar impression. In all five cases, the lesion occurred in the cervical spinal cord.

Results of preoperative MR imaging revealed a variable degree of enlargement of the cervical cord in all patients. All patients had abnormal T1 and T2 prolongation of the cervical spinal cord signal extending over a variable distance. The T1 signal was not as low as CSF in any case, and the margins of the T1 signal abnormality were not sharply defined. No frank cavitation was observed in any pa-

TABLE 1: Continued.

MR Findings Pre-Op	Surgical Intervention	Clinical Findings Post-op	MR Findings Post-op
Progressive T1 and T2 prolongation within upper cervical cord; no cavity; tonsillar herniation with reduced CSF flow at FM	Aggressive suboccipital decompression and partial resection of cerebellar tonsils	Improved headaches, decreased clumsiness	Near-resolution of T1 and T2 prolongation in cord substance, improved CSF flow at FM
Marked enlargement of mid-cervical cord; T1 and T2, prolongation from C3–C4 to T1–T2; large ventrolateral osteophyte at C3–C4 level	C3 through C7 laminectomy, lysis of subdural adhesions, and sectioning of dentate ligaments at C3 and C4	Substantial improvement in strength, sensation in arms and legs within hours after surgery	Decrease in cord caliber, persistent T1 and T2 prolongation below C3–C4 level, where the cord remains focally adhesed
Cord enlargement from C1 to T3, with T1 and T2 prolongation	C6 and C7 laminectomy with exploration and myelotomy but no shunt as a syrinx cavity was not found	Slight improvement in right hand function, decreased neck and arm pain	Progressive decrease in cord enlargement and T1 and T2 prolongation, then late decline and progression to frank syrinx formation
Cervical cord enlargement with T1 and T2 prolongation, enlarged ventricles with tonsillar herniation	VP shunting to relieve hydrocephalus	Improved mental status, decreased neck stiffness, resolution of quadriparesis	Complete resolution of cord enlargement and signal abnormalities
Severe cervical spondylostenosis, basilar impression, and atlantoaxial subluxation; cord enlargement and edema from cervicomedullary junction to C6–C7	C1 to C6 laminectomies with medial facetectomies, then posterior fusion from C4 to C6	Stabilization of neurologic findings, mild improvement in lower extremity spasticity	Decreased cord enlargement and significant decrease in cord signal abnormality

tient. Mild parenchymal enhancement of the upper cervical cord was observed in one case; this patient had no evidence of an acute clinical decline or systemic infectious or inflammatory condition, and her CSF profile was benign.

Evidence of a discrete level of obstruction to normal CSF flow was detected preoperatively in all but one patient. Patient 1 (Fig 1) had a Chiari I malformation with markedly narrowed CSF spaces at the level of the foramen magnum; a cine phase-contrast CSF flow study showed markedly restricted flow of CSF through the foramen magnum. Patient 2 (Fig 2) underwent preoperative CT myelography that showed a decreased flow of contrast material around a swollen cervical spinal cord and a myelographic block at the C3–C4 level caused by a large ventrolateral osteophyte and possibly adhesions as well; subtle increased density of the cord on delayed images was also found. Patient 4 (Fig 3) had a markedly enlarged fourth ventricle and tonsillar herniation that resulted in obstruction to flow at the level of the foramen magnum. Patient 5 had multilevel spondylostenosis and marked compression at the level of the foramen magnum caused by basilar impression and atlantoaxial subluxation. In all these cases, the level of obstruction was rostral to the level of cord signal changes. The level of obstruction in patient 3 was not clear preoperatively; this patient had a history of previous posterior fossa surgery and basilar adhesions that were most likely causing obstruction to flow at the level of the foramen magnum, but he also had a mild congenital spinal stenosis with superimposed acquired stenosis at the C5–C6 and C6–C7 levels. In this case, it is unclear whether the spinal cord signal changes were only caudal or both rostral and caudal to the level of obstruction to CSF flow.

Four of five patients underwent surgical intervention directed at restoring patency of CSF pathways. Patient 3 (Fig 4) underwent laminectomy and intradural exploration for placement of a syringopleural shunt, but this procedure was aborted because no syrinx was found (see below). Procedures performed are summarized in the Table. Only patient 3 underwent intraoperative sonographic evaluation of the spinal cord. Postoperatively, all patients experienced clinical improvement to varying degrees.

Postoperative MR imaging was performed in all patients from 1 week to 1 year after surgery. In all cases, the postoperative images showed a reduction in cord caliber, as well as improvement or resolution of T1 and T2 signal abnormalities. One patient (patient 3, Fig 4) experienced a subsequent deterioration in his clinical status after having had some improvement in clinical and imaging findings in the immediate postoperative period after lower cervical laminectomy and myelotomy. A second postoperative image 6 weeks after surgery showed an increase in central parenchymal T2 prolongation. No definite evidence was found for recurrent CSF obstruction at the surgical level, but the cord remained deformed at the level of the foramen magnum, and it was considered likely that obstruction to normal CSF flow remained at the foramen magnum level that had not been addressed surgically; a cine phase-contrast CSF flow

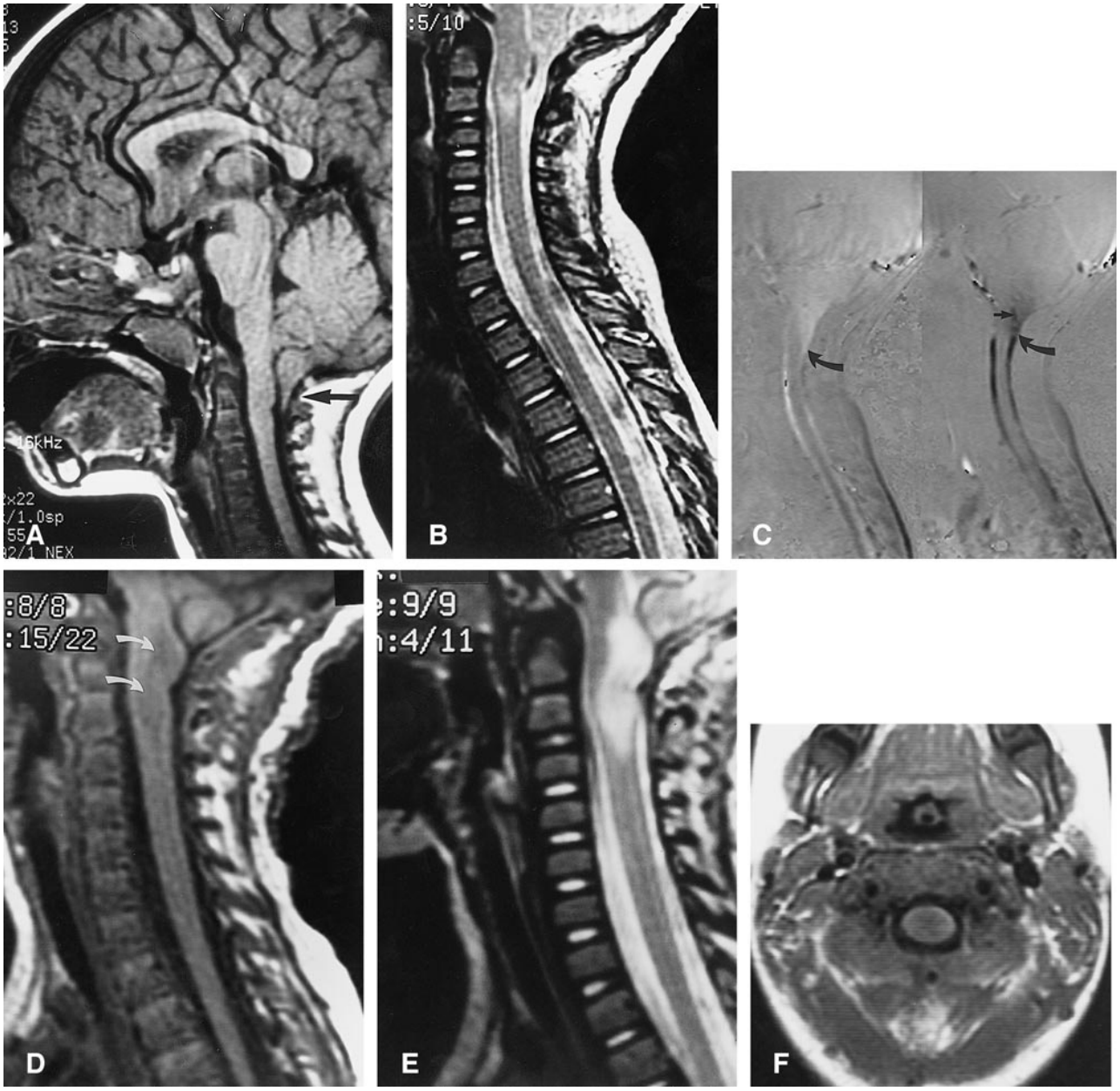

study was not performed at this time, because this sequence was unavailable at the rehabilitation hospital where the patient was imaged. No further intervention was undertaken after that study for psychosocial reasons, and the patient was reexamined by his neurosurgeon 10 months later, because of symptom progression. A third postoperative study at this time revealed progression to frank syrinx formation. At this time, a syringopleural shunt was easily placed, but the patient experienced only minimal symptomatic improvement.

Discussion

The understanding of the pathogenesis of syringomyelia has been advanced by the important pathologic studies of Milhorat et al (7, 27, 28). On the basis of detailed histopathologic findings, they distinguished among three types of spinal cord cavities: 1) dilatations of the central canal that communicate directly with the fourth ventricle (communicating syrinxes); 2) noncommunicating dilatations of the central canal that arise below a syrinx-free segment of spinal cord; and 3) extracanalicular syrinxes that originate in the spinal cord parenchyma and do not communicate with the central canal. By correlating with clinical parameters, they were able to associate these distinct cavitary patterns with different mechanisms of pathogenesis. Communicating syrinxes were found in association with hydrocephalus and were caused by obstruction of CSF circulation distal to the outlets of the fourth ventricle. Noncommunicating syrinxes were associated with disorders of CSF dynamics in the spinal subarachnoid space, such as the Chiari I

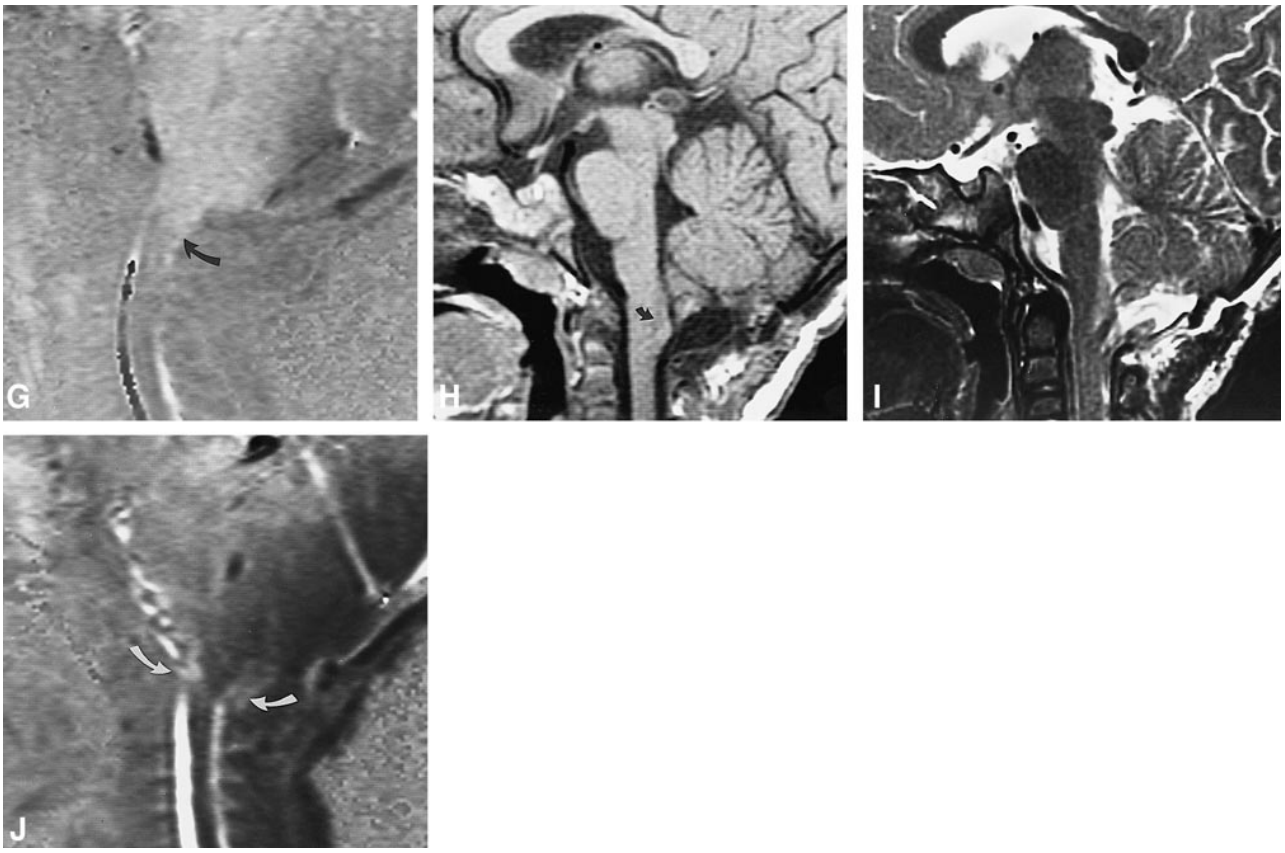

FIG 1. Patient 1.

A, Sagittal T1-weighted image (600/8/2) shows a Chiari I malformation, with tonsillar herniation to the mid-C2 level and a pointed configuration to the cerebellar tonsils (*arrow*).

B, Sagittal T2-weighted image ($3000/105_{eff}/3$) shows T2 prolongation within the spinal cord parenchyma at the C2–C3 level.

C, Sagittal images from a cine phase-contrast flow study in systole (*left panel*) and diastole (*right panel*), sensitized to flow in the superior-to-inferior direction (see text for parameters). Note the absence of flow-related phase change at the level of the foramen magnum, as well as prominent tonsillar motion in both systole and diastole, with the *curved arrows* indicating the position of the tonsillar tips in systole and diastole. Subtle linear low signal is present anterior to the tonsil in diastole (*right panel*, *straight arrow*), indicating minimal flow between the fourth ventricle and the spinal subarachnoid space below the level of the foramen magnum.

D, Sagittal T1-weighted image (500/14/3) obtained 6 weeks later after limited extradural decompression of the foramen magnum. Cord expansion and parenchymal hypointensity (*curved arrows*) are present in the upper cervical cord.

E, Sagittal T2-weighted image ($3000/105_{eff}/3$) corresponding to *D* shows marked upper cervical cord T2 prolongation. This was presumed related to ongoing or increased obstruction to CSF flow.

F, Axial T1-weighted image (500/13/2) shows that the central parenchymal signal abnormality is somewhat ill-defined and not as low in signal intensity as CSF.

G, Cine phase-contrast flow study sensitized to motion in the superior-to-inferior direction (see text for parameters) shows prominent downward motion of the brain stem and cerebellar tonsils (which appear white), but no definite flow of CSF at the foramen magnum. The tip of the tonsil is indicated (*curved arrow*).

H, Sagittal T1-weighted image (600/8/2) after aggressive decompression of the foramen magnum, including duraplasty, lysis of arachnoid adhesions, and partial tonsillar resection shows that the upper cervical cord appears to be of normal caliber. Minimal parenchymal hypointensity persists in the upper cervical spinal cord (*curved arrow*).

I, Sagittal T2-weighted image ($4000/105_{eff}/2$) corresponding to *H* shows near-complete resolution of previously seen abnormal T2 prolongation.

J, Cine phase-contrast flow study sensitized to motion in the superior-to-inferior direction (see text for parameters) no longer shows abnormal downward motion of the brain stem or residual cerebellar tonsils. CSF flow is evident at the foramen magnum (*curved arrows*).

malformation, cervical spinal stenosis, basilar impression, and arachnoiditis. Extracanalicular or parenchymal syrinxes were typically found in the watershed area of the spinal cord, associated with conditions that cause direct injury to spinal cord tissue, such as trauma, infarction, and hemorrhage. Additionally, they found that concentrically enlarged central cavities (as are seen with communicating or noncommunicating syrinxes) either were asymptomatic or were associated with bilateral, nonspecific neurologic findings, such as spasticity, weakness, and segmental pain.

The theory that noncommunicating syringomyelia is related to alterations in CSF flow has received experimental support. The findings of several groups of investigators (20–22, 24) have shown in animal models that, under normal circumstances, CSF flows from the spinal subarachnoid space into perivascular spaces of the spinal cord and, from there, along the interstitial spaces toward

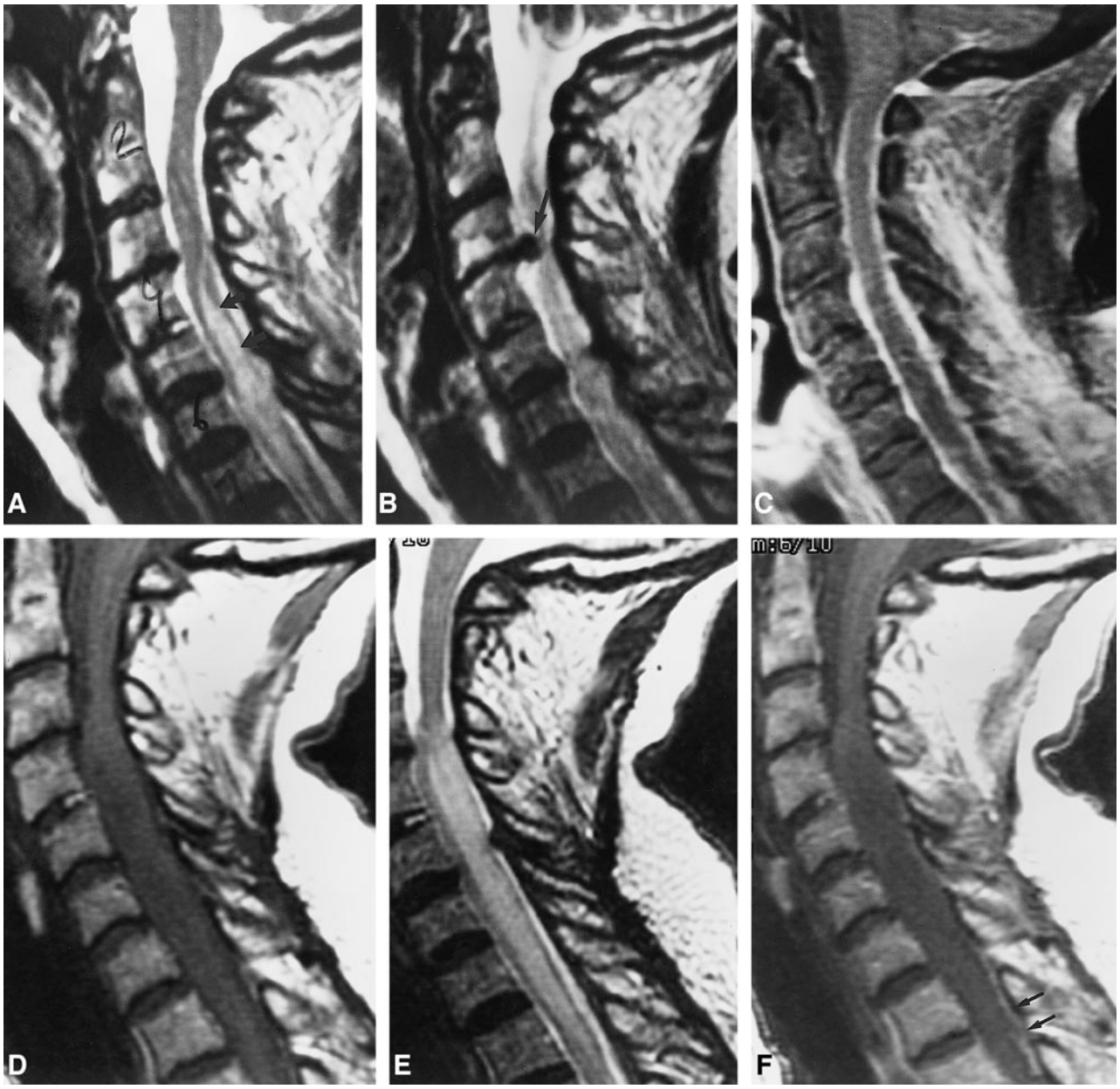

the central canal. This net unidirectional flow is hypothesized to be driven by both pulsatile and bulk mechanisms (23), although it is unclear whether the impetus to flow is actual arterial pulsations within the spinal cord or the transmission of intracranial arterial pulsations to the CSF in the spinal subarachnoid space. Both accentuation of arterial pulsations during systole as well as redirection and accentuation of CSF pulsations transmitted through the subarachnoid space are theorized to account at least in part for the formation and expansion of cysts in noncommunicating types of syringomyelia, although additional experimental work is necessary to investigate these hypotheses. The role of adhesive arachnoiditis in syrinx formation has also been investigated experimentally (17). Subarachnoid block caused by adhesive arachnoiditis may initiate the formation or enlargement of a syringomyelic cavity, perhaps by redirecting and/or accentuating transmission of the force of systolic arterial pulsations.

The development of noncommunicating syringomyelia, or focal central canal dilatation remote from the site of CSF obstruction, may relate to variations in the patency of the central canal among individuals. The findings of Milhorat et al (7) showed that noncommunicating syrinxes were defined rostrally as well as caudally by stenosis of the central canal. An autopsy study of 232 patients without spinal cord abnormalities by this same group (29) indicated that stenosis of the central canal correlates with the age of the patient. Varying degrees of stenosis were present at one or more levels in 3% of infants under 1 year of age, 88% of adolescents and young adults

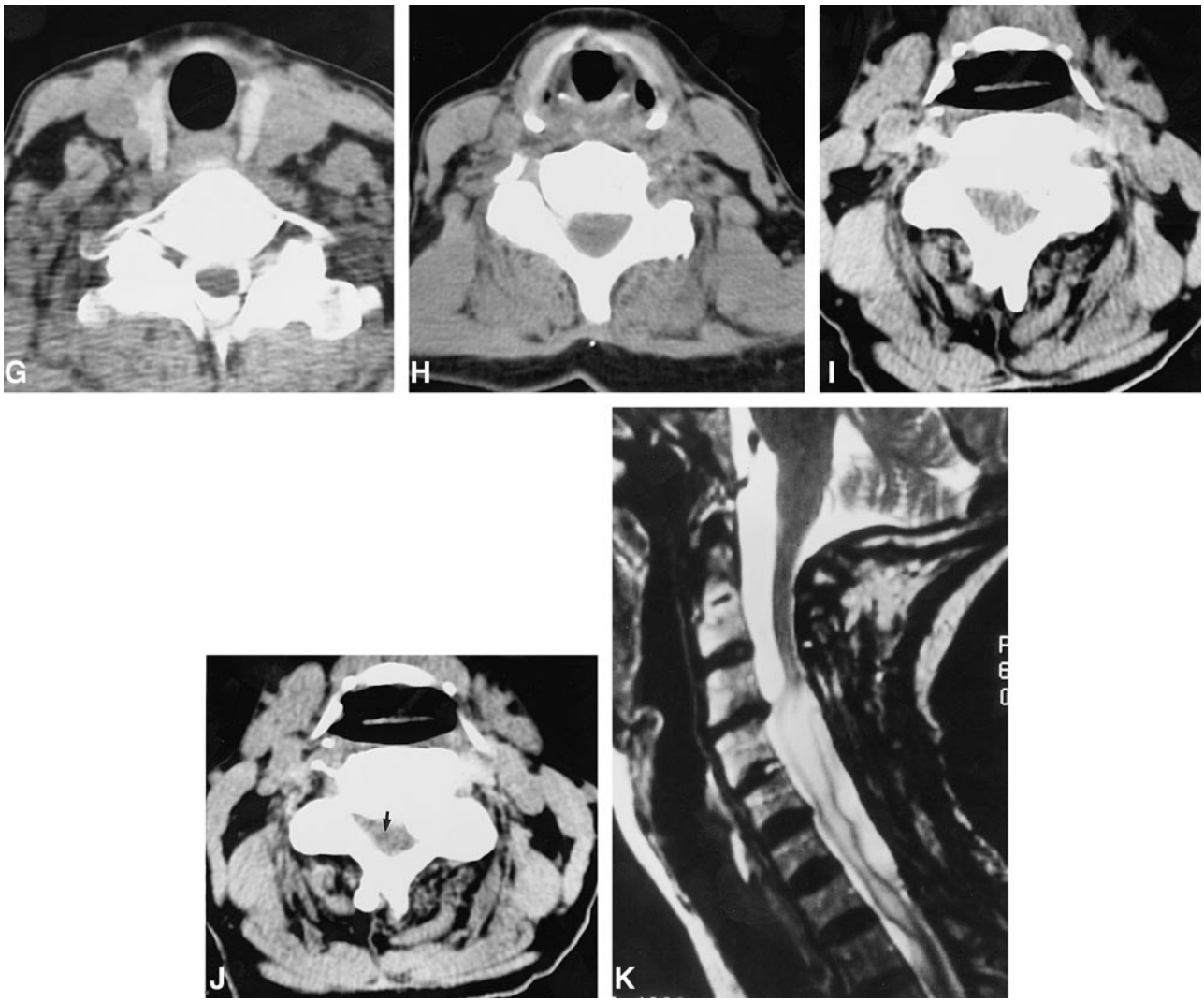

FIG 2. Patient 2.

A, Midline sagittal T2-weighted image (4000/102$_{eff}$/2) shows central T2 prolongation within the lower cervical spinal cord parenchyma (*arrows*).

B, Parasagittal T2-weighted image (4000/102$_{eff}$/2) shows a large paracentral disk/osteophyte complex at the C3–C4 level (*arrow*).

C, Contrast-enhanced sagittal T1-weighted image (650/15/2) with fat saturation shows intense meningeal enhancement along the surface of the spinal cord. The patient was treated aggressively with broad-spectrum antibiotics and a decompressive laminectomy at C6 for a parasagittal epidural abscess (not shown).

D, Sagittal T1-weighted image (600/11/3) obtained 16 months later shows marked enlargement of the cervical spinal cord below the C3–C4 level. The parenchyma is hyperintense compared with CSF, and no evidence is detected of frank cavitation.

E, Sagittal T2-weighted image (4000/102/2) confirms the marked enlargement of the cervical cord below the C3–C4 level as well as extensive and confluent T2 prolongation within the central cord parenchyma. The cord surface is slightly irregular at C3–C4, suggesting possible adhesions.

F, Contrast-enhanced sagittal T1-weighted image (650/11/2) shows no abnormal enhancement of the cord parenchyma. Faint linear increased signal dorsal to the cord (*arrows*) likely represents residual thickening and fibrosis of the dura/epidural space related to the previous intense inflammatory episode.

G, Cervical CT myelogram was obtained several days later, via a lumbar approach. Axial image at the C7–T1 level shows normal-appearing spinal cord surrounded by dense intrathecal contrast.

H, Axial image from the CT myelogram at the C5–C6 level shows marked cord enlargement and minimal intrathecal contrast along the right lateral cord.

I, Axial image from the CT myelogram at the C3–C4 level shows a narrow spinal canal, a left lateral calcified disk/osteophyte complex, and a lack of contrast around the spinal cord.

J, Delayed CT scan obtained 6 hours after the initial study shows subtle increased density of the peripheral parenchyma at the C3–C4 level consistent with penetration of contrast medium. The central cord (*arrow*) stands out in subtle contrast to the more dense peripheral white matter.

K, Postoperative sagittal T2-weighted image (4000/102$_{eff}$/2) obtained after C3 to C7 laminectomy, lysis of subdural adhesions, and sectioning of the dentate ligaments at C3 and C4 shows a marked decrease in cord caliber. Parenchymal T2 prolongation persists, as does irregularity consistent with persistent adhesions/obstruction at the C3–C4 level. Because the patient was symptomatically improved, it was elected to monitor her with serial imaging studies rather than to reoperate.

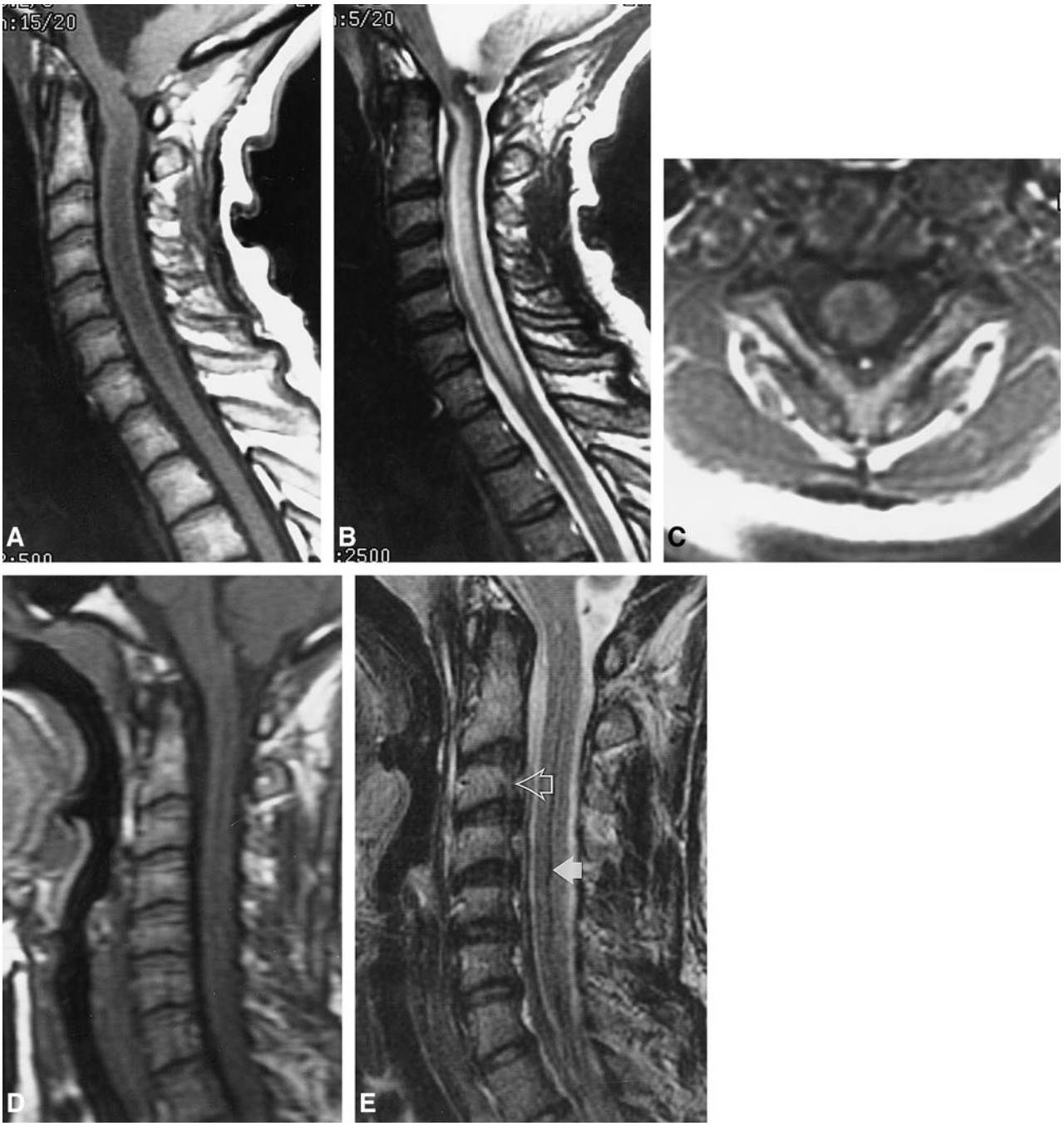

FIG 3. Patient 4.

A, Sagittal T1-weighted image (500/15/2) shows enlargement of the cervical cord and central parenchymal hypointensity. There is marked enlargement of the fourth ventricle and secondary tonsillar herniation with crowding of the foramen magnum.

B, Sagittal T2-weighted image ($2500/102_{eff}/2$) shows striking T2 prolongation within the central portion of the cord.

C, Axial T1-weighted image (583/17/2) at the C2–C3 level shows that the central cord hypointensity has an irregular margin and is not isointense with CSF.

D, Sagittal T1-weighted image (500/14/1.5) after treatment of hydrocephalus. The fourth ventricle is decompressed, the cerebellar tonsils are normally positioned, and cord caliber has returned to normal.

E, Sagittal T2-weighted image ($2500/102_{eff}/2$) shows complete resolution of previously noted parenchymal T2 prolongation. A dark line down the center of the cord (*solid arrow*) is presumably artifactual because of patient motion and/or truncation artifact, as other parallel lines (*open arrow*) are observed across the image.

(ages 13 to 29 years), and 100% of those over age 65. They concluded that the frequency and extent of central canal stenosis in humans almost certainly affects the clinical features of syringomyelia. Theoretically, a disturbance of CSF circulation in the spinal subarachnoid space redirects fluid through the interstitial spaces of the spinal cord and eventually into a patent segment of the central canal. Focal obliteration of the central canal above this level prevents communication between the syrinx and the fourth ventricle, initiating the conditions required for establishment of noncommunicating syringomyelia.

Clinical studies also support the importance of CSF flow patterns and subarachnoid space pressure waves in the initiation and propagation of syringomyelia. Oldfield et al (19) studied seven patients with Chiari I malformations and syringomyelia using MR imaging and intraoperative sonography. On the basis of their observations, they suggest that the development and progression of noncommunicating syrinxes associated with the Chiari I malformation are caused by obstruction to the normal rapid to-and-fro movement of CSF across the foramen magnum by tonsillar ectopia and the ventral position of the lower brain stem. During systole in the Chiari I malformation, brain expansion is accommodated by abrupt caudal movement of the tonsils. This downward, pistonlike systolic tonsillar movement can be shown on direction-sensitive cine phase-contrast MR sequences (Fig 1C). Rapid downward tonsillar movement, perhaps in concert with the deposition of fourth ventricular CSF into the spinal subarachnoid space below the level of obstruction, imparts an accentuated systolic pressure wave into the upper cervical spinal canal, forcing CSF into spinal cord parenchyma during systole. Oldfield et al (19) believed that their hypothesis might explain the origin and progression of noncommunicating syrinxes associated with the hindbrain malformations, as well as with other conditions that obstruct CSF flow in the spinal subarachnoid space, such as arachnoiditis and extramedullary tumors.

Syringomyelia is commonly observed in the posttrauma setting (1–3). In the case of trauma, the inciting event for syrinx formation is focal cord injury, although the propagation of a posttraumatic syrinx may certainly be related at least in part to alterations in CSF flow (30). In trauma patients, a condition termed progressive posttraumatic myelomalacic myelopathy (PPMM) has been described that is considered to represent a continuum of interrelated disease processes that may precede formation of a confluent cyst (31). Patients with PPMM are generally clinically indistinguishable from those with cystic myelopathy, and, in some cases, have been reported to have a microcystic myelopathy (30–35). The presence of localized arachnoiditis at the level of trauma leading to spinal cord tethering is considered to play an important role in the pathophysiology of PPMM, related at least in part to changes in local CSF dynamics (30, 31). Analogous to the situation of PPMM, our patients had myelopathic symptoms associated with conditions that predisposed them to syrinx formation, and, on MR images, had cord abnormalities without definite syrinx formation. To our knowledge, this has not been documented in patients without a history of trauma.

Specifically, the underlying conditions in our patients included Chiari I malformation, cervical spondylostenosis, and arachnoiditis, all of which are associated with both impedance to normal CSF flow and syrinx formation. All of our patients had nonspecific myelopathic symptoms, similar to patients with noncommunicating syringomyelia described by Milhorat et al (28), and had findings on MR images similar to those seen in cases of progressive posttraumatic myelomalacic myelopathy (31), including cord enlargement and T1 and T2 prolongation, with the T1 signal not as low as that of CSF and not sharply marginated. In the distinction between cystic and noncystic myelopathy, proton density–weighted images may be useful, since a cyst would be expected to be isointense with CSF whereas myelomalacic or microcystic changes would likely be hyperintense (36); however, proton density–weighted images may not be completely reliable, since a cyst may be hyperintense relative to CSF on a proton density–weighted image because of dampened CSF pulsations or a slightly elevated protein content. In addition, with the advent of fast spin-echo imaging of the spine, double-echo spin-echo sequences have been dropped from many imaging protocols, and we do not perform them routinely at our institution. Axial T1-weighted images may also be useful in the distinction of cystic from noncystic changes. Intraoperative sonography is certainly a useful adjunct in the assessment of cystic versus noncystic myelopathy (31, 34, 37, 38), but the performance of this examination varies among institutions and among individual surgeons and requires surgical exposure.

Findings strongly supporting disturbance of CSF flow were observed on preoperative imaging studies in four of our five patients, and the surgical procedures performed were either directed at restoring patency of CSF pathways or had that end effect in all patients. We do not have direct information on the status of the central canal in our patients, but we hypothesize that it was not patent, and, thus, CSF that was driven into the spinal cord parenchyma by alterations in normal flow patterns was unable to enter the central canal to form a syrinx (Figs 5 and 6). After improvement or reconstitution of CSF pathways, all patients experienced stabilization or improvement in clinical symptoms. Additionally, results of postoperative MR examinations showed both a reduction in cord caliber and an improvement in cord parenchymal signal abnormalities. Whether the signal alterations represent edema or microcystic change or both is unclear, since pathologic specimens are not available from these patients. A direct traumatic injury to the cord

does not seem to be a necessary prerequisite for the development of this condition. A difficulty with this hypothesis is explaining the later development of frank cavitation in patient 3; however, it is possible that partial recanalization of the central canal may have occurred, followed by paracentral dissection around a stenotic segment (29). Alternatively, the myelotomy performed during the initial surgery may have created a pathway along which a syrinx could form and then extend.

Jinkins et al (39) recently described three patients with clinically progressive posttraumatic syringomyelia in whom extensive MR signal change on T2-weighted images in the spinal cord superior to a well-defined syrinx was found to be an ancillary sign of disease progression. After shunting of the syrinx, the

FIG 4. Patient 3.

A, Sagittal T2-weighted image ($4000/108_{eff}/4$) obtained when the patient had no symptoms referable to the spinal cord shows a mild dilatation of the obex/proximal central canal and central T2 prolongation within the upper cervical cord parenchyma.

B, Sagittal T1-weighted (*left panel*) (600/11/2) and T2-weighted (*right panel*) ($3000/96_{eff}/2$) images obtained 1 year later when the patient had developed progressive neck pain and spastic quadriparesis show striking cord expansion and both T1 and T2 prolongation within the cervical spinal cord. The areas of abnormal signal within the cord approach, but are not quite equal to, CSF in intensity.

C, Axial T1-weighted image (650/9/3) shows irregularly marginated central parenchymal hypointensity, although this area is hyperintense compared with CSF in the spinal canal. These images (*A–C*) were interpreted as consistent with syrinx by the neurosurgeon, and the patient was taken to the operating room for shunt placement. Intraoperatively, the cord was noted to be enlarged and ''boggy.'' A myelotomy was performed at the C6 level, and a small amount of fluid exuded from the cord surface, but no syrinx was encountered. Intraoperative sonogram (not shown) confirmed the lack of frank cavitation.

D, Sagittal T2-weighted image ($3500/96_{eff}/3$) obtained 2 days postoperatively shows evidence of recent C6–C7 laminectomy. The cord is notably reduced in overall caliber compared with the preoperative study, and the signal has normalized at the myelotomy site (*arrow*).

E, Repeat T2-weighted image ($2500/105_{eff}/3$) obtained 8 days later shows further regression of signal abnormality and further reduction of cord caliber.

F, Sagittal T2-weighted image ($3894/112_{eff}/1$) obtained 1 month later shows an increase in central T2 prolongation within the cervical spinal cord, as well as an increase in cord caliber. The patient was doing fairly well in rehabilitation and did not desire further intervention. The patient was lost to follow-up for 10 months.

G, Sagittal T1-weighted image (500/8/3) obtained 11 months after surgery shows further enlargement of the cervical and upper thoracic spinal cord. The cord centrally is hypointense, and multiple septations are present (*arrow*) consistent with syringomyelia. The patient clinically was severely quadriparetic and had lost control of bowel and bladder function. After this image, surgery was performed, during which a large syrinx was encountered and a syringopleural shunt was placed (not shown).

parenchymal T2 hyperintensity resolved, and neurologic deficits stabilized or improved. They postulated that the T2 hyperintensity represented fluid escaping from the cyst or edema caused by as yet undefined pathologic alterations in the spinal cord adjacent to the cyst. In these cases, a definite obstruction to flow of CSF was not described, and the intervention taken (syrinx shunting) was not aimed at restoring patency of CSF pathways. It is possible that the enlarged cord caused relative obstruction of normal CSF flow pathways, resulting in a ''presyrinx'' condition cranial to the already formed syrinx cavity.

In further support of our hypothesis, the reversibility of cord signal abnormality associated with obstruction to normal CSF flow has been reported in a case of acquired tonsillar herniation caused by probable spontaneous intracranial hypotension (40–42). In this case, the cervical cord was enlarged and had T1 and T2 prolongation without frank cavitation, consistent with the presyrinx state. After spontaneous resolution of the patient's condition (presumably because of closure of an occult CSF leak), the cerebellar tonsils returned to a normal position, and the cervical cord caliber and signal reverted to normal. The patient was not myelopathic but did experience occipital and neck pain. The lack of myelopathic symptoms is not inconsistent with presyrinx physiology, since even patients with frank syringomyelia (typically of the central cavitary type) may be asymptomatic (28).

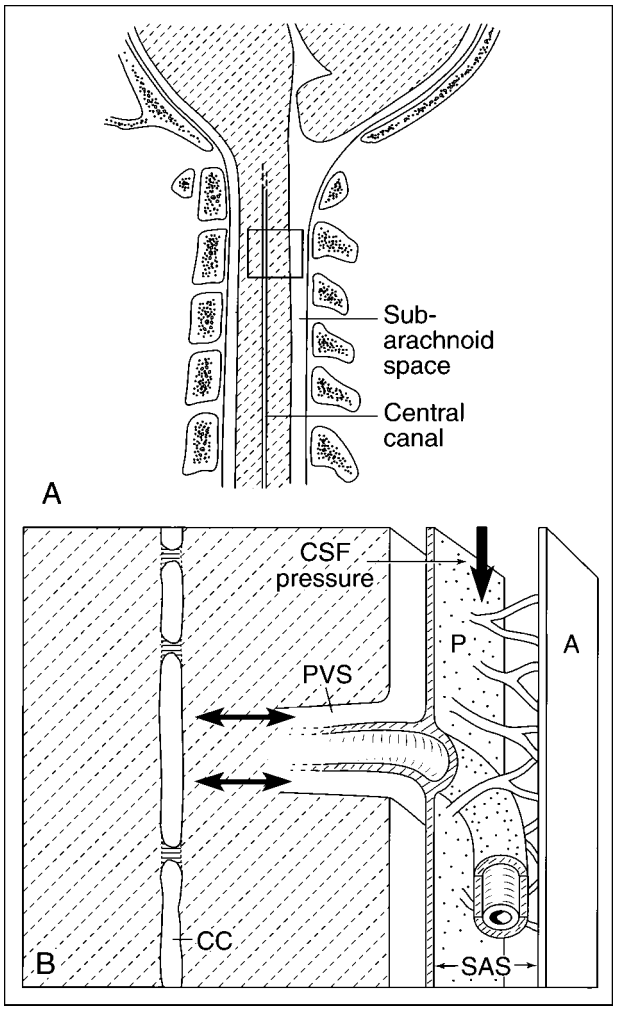

FIG 5. Diagrammatic representation of CSF flow under normal circumstances.

A, Sagittal view of the craniocervical junction and upper cervical spinal cord in an anatomically normal patient shows no obstruction to CSF flow at the foramen magnum. A segment of spinal cord parenchyma (*box*) is shown in more detail in *B*.

B, Magnified view of the *box* in *A* shows CSF flow dynamics in a normal patient with a variably stenotic central canal (CC) (29), as indicated by the *horizontal lines*. CSF pressure (*vertical arrow*) is normal. CSF flows from the subarachnoid space (SAS) between the arachnoid (A) and pia (P) to the subpial space, and then enters the perivascular space (PVS). CSF circulates through the cord parenchyma toward the central canal, but may also flow in reverse, as these forces are relatively balanced under normal circumstances (*double-headed arrows*) (45, 46).

Because surgical intervention was performed that restored or improved CSF flow pathways in all our patients, we are unable to prove that they would have progressed to frank syrinx formation. The implication that syrinx formation would have occurred if the patients were left untreated is justified by the following three considerations: first, the underlying conditions in our patients all have a known association with syringomyelia; second, in one patient (patient 3) who initially responded to surgical intervention with marked improvement in cord enlargement and signal abnormality, clear-cut syrinx formation occurred during the follow-up period, presumably because the underlying obstruction to CSF flow had not been fully addressed by the surgical procedure performed; and third, the recent observations of Jinkins et al (39), which suggest that reversible T2 changes were considered to predict frank syrinx formation. We, therefore, propose the use of the term ''presyrinx'' state as a valid concept to describe these and similar cases.

We have also considered other possible causes of the reversible cord enlargement and T2 prolongation identified in our patients. It seems unlikely that arterial ischemia plays a significant role in the pathogenesis of the presyrinx state based on the fact that the imaging abnormalities did not conform to a vascular territory and were reversible as assessed by postoperative imaging. Venous ischemia could have played a role in cord enlargement and signal changes, analogous to the pathophysiology of spinal dural arteriovenous fistula, but no abnormal veins were identified at preoperative imaging or intraoperatively. The lack of identification of macroscopic abnormal veins does not, however, exclude a role for venous ischemia. In the setting of trauma, occluded intramedullary veins have been identified in degenerated segments of spinal cord (43). In the nontraumatic setting, it is possible that pressure changes in the epidural venous plexus in association with disturbances of CSF circulation lead to an increase in spinal venous pressure and accumulation of fluid in the spinal cord (12). Venous ischemic changes are also known to be reversible. However the venous drainage of the spinal cord is quite rich, and the mechanism by which venous ischemia would have occurred in our patients is not clear. Therefore, although we propose that the presyrinx state is fundamentally one of altered CSF flow parameters, we do recognize that a contribution of venous ischemia may be present as well and that sorting out these relationships will require further study.

The relationship between the level of the block to CSF flow and the location of the presyrinx lesion also warrants consideration. As most of our patients had high cervical or foramen magnum blockages to CSF flow, it is not surprising that the spinal cord parenchymal signal changes that we observed developed caudal to the block. Pathophysiologically, this is most likely related to fluid entering the cord below the level of the block and then tracking cephalad in cord parenchyma and/or the central canal to circumvent the block; however, in the experience of Jinkins et al (39), which we consider an analogous situation, the presyrinx lesion extended rostral to the level of obstruction. In the setting of trauma, syrinxes most commonly extend superiorly from the site of injury, although superior and inferior extension, and even inferior extension alone, have been observed. This may relate to the fact that the cervical cord expands more easily than the thoracic cord (3, 9, 44).

An important but as yet unexplained aspect of this phenomenon is why we do not see these MR findings more frequently in cases of Chiari I malformations and basal arachnoiditis, as these are not

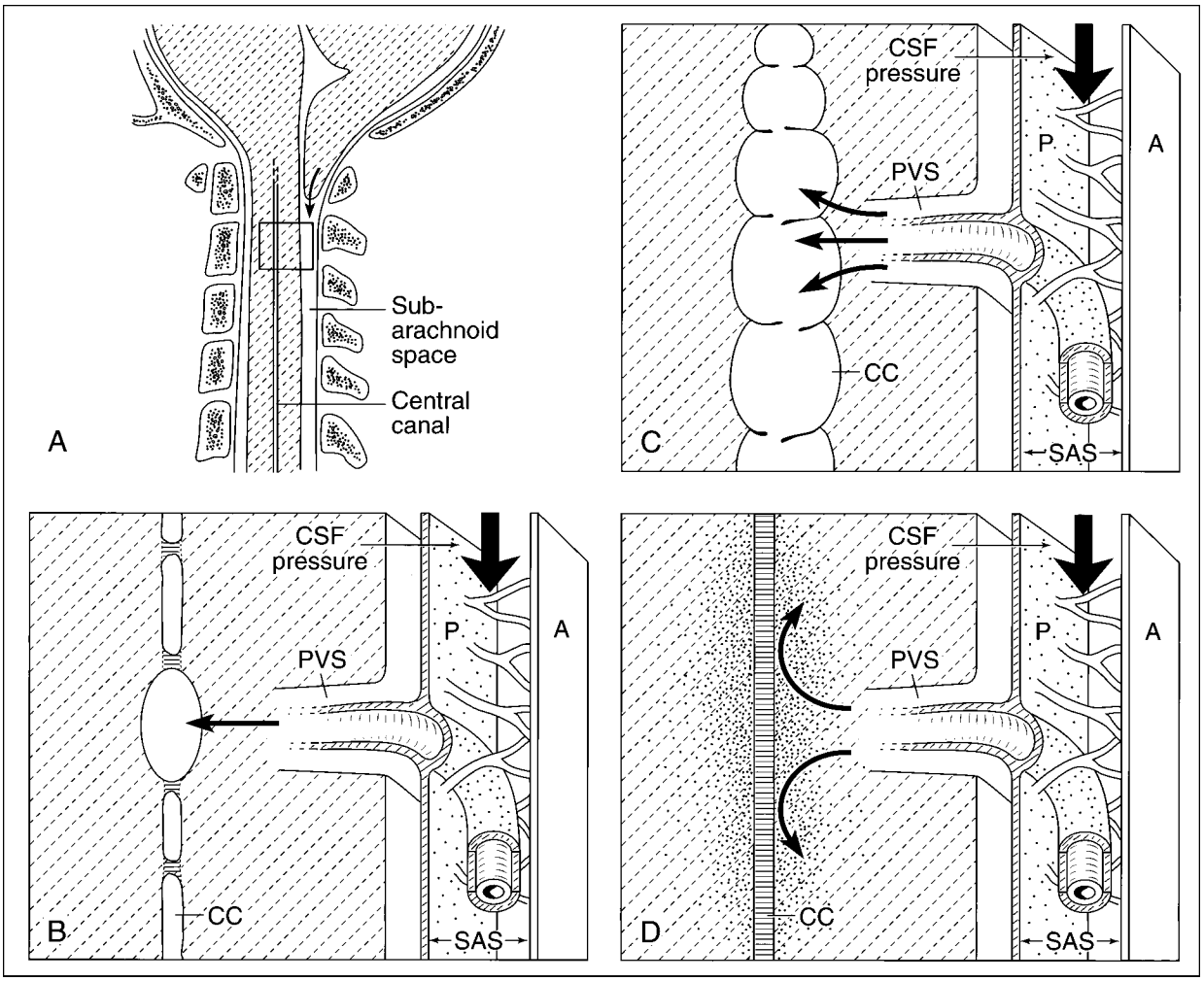

FIG 6. Diagrammatic representation of syringomyelia and the ''presyrinx'' hypothesis in the setting of obstruction to CSF flow.

A, Sagittal view of the craniocervical junction in a patient with a Chiari I malformation shows abnormal descent of the cerebellar tonsil below the level of the foramen magnum (*arrow*). A segment of spinal cord parenchyma (*box*) is magnified in *B* to *D*, which represent views of CSF dynamics at the level of the spinal cord parenchyma in the presence of alterations in normal CSF flow and variable patency of the central canal.

B, Focal noncommunicating syrinx. In the setting of a Chiari I malformation and a variably stenotic central canal (which is a normal variant in many adults), as the tonsils descend rapidly during systole, CSF is driven into the spinal cord parenchyma by increased CSF pressure (*thick vertical arrow*). Net CSF flow occurs toward the central canal, resulting in focal syringomyelia, which is limited in its craniocaudal extent by intervening stenosis of the central canal. CC = central canal, A = arachnoid, P = pia, SAS = subarachnoid space, PVS = perivascular space.

C, Extensive noncommunicating syrinx. This situation is similar to *B*, but the central canal is more extensively patent. In this situation, a long-segment dilatation of the central canal occurs as CSF is driven into the central canal (*curved arrows*) via the perivascular spaces by the accentuated CSF pulse pressure (*thick vertical arrow*) that results from the downward motion of the low-lying cerebellar tonsils in systole.

D, ''Presyrinx.'' In the setting of altered CSF flow, as with a Chiari I malformation, fluid in the subarachnoid space is subjected to increased pressure (*thick vertical arrow*). Net CSF flow is into the spinal cord parenchyma; however, because the central canal is not patent (as indicated by the *horizontal lines*), fluid cannot accumulate within the central canal (*curved arrows*) and, therefore, diffuses through the cord parenchyma (*stippled area*), resulting in cord enlargement and edema.

uncommon conditions. Because patients in the presyrinx state may have minimal clinical symptoms or even be asymptomatic, they may not come to medical attention until frank cavitation and more severe symptoms have developed. Additionally, a dynamic balance between CSF pressure in the spinal subarachnoid space and the spinal cord parenchyma may exist, and the anatomic conditions required to establish the presyrinx state may occur only rarely. For instance, the establishment of this state may depend on the morphology and extent of the network of spinal perivascular spaces and the capacity and patency of the central canal, among other factors. Intervention at an appropriate time may allow restoration of normal flow patterns and reversal of parenchymal signal abnormalities, as well as improvement in neurologic deficits. That this entity may represent an equilibrium state is supported by the documentation of this appearance in one of our patients (patient 2) for some time before she progressed symptomatically to the point that surgical intervention was performed. Further

study will be necessary to better understand normal and abnormal spinal subarachnoid fluid circulation and the pathophysiology of syrinx formation.

Conclusion

We have described a condition of reversible spinal cord enlargement and T1 and T2 prolongation, the ''presyrinx'' state, which occurs in the setting of CSF flow obstruction and may be misinterpreted as syringomyelia on MR studies. Surgical intervention aimed at restoring patency of CSF pathways is likely to be of benefit in these patients, and MR findings should guide selection of the procedure to be performed. This entity presumably represents a point on the continuum to development of syringomyelia and may be pathophysiologically related to variations in the patency of the central canal and also to the entity of progressive posttraumatic myelomalacic myelopathy.

References

1. Rossier AB, Foo D, Shillito J, Dyro FM. **Posttraumatic cervical syringomyelia.** *Brain* 1985;108:439–461
2. Vernon JD, Silver JR, Ohry A. **Posttraumatic syringomyelia.** *Paraplegia* 1982;20:339–364
3. Quencer RM, Green BA, Eismont FJ. **Posttraumatic spinal cord cysts: clinical features and characterization with metrizamide computed tomography.** *Radiology* 1983;146:415–423
4. Gardner WJ. **Hydrodynamic mechanism of syringomyelia: its relationship to myelocele.** *J Neurol Neurosurg Psychiatry* 1965;28: 247–259
5. Williams B. **The distending force in the production of "communicating syringomyelia."** *Lancet* 1969;2:189–193
6. Ball MJ, Dayan AD. **Pathogenesis of syringomyelia.** *Lancet* 1972; 2:799–801
7. Milhorat TH, Capocelli AL, Anzil AP, Kotzen RM, Milhorat RH. **Pathological basis of spinal cord cavitation in syringomyelia: analysis of 105 autopsy cases.** *J Neurosurg* 1995;82:802–812
8. Caplan LR, Norohna AB, Amico LL. **Syringomyelia and arachnoiditis.** *J Neurol Neurosurg Psychiatry* 1990;53:106–113
9. Klekamp J, Batzdorf U, Samii M, Bothe HW. **Treatment of syringomyelia associated with arachnoid scarring caused by arachnoiditis or trauma.** *J Neurosurg* 1997;86:233–240
10. Brammah TB, Jayson MIV. **Syringomyelia as a complication of spinal arachnoiditis.** *Spine* 1994;19:2603–2605
11. Phanthumchinda K, Kaoropthum S. **Syringomyelia associated with post-meningitis spinal arachnoiditis due to Candida tropicalis.** *Postgrad Med J* 1991;67:767–769
12. Klekamp J, Samii M, Tatagiba M, Sepehrnia A. **Syringomyelia in association with tumors of the posterior fossa: pathophysiological considerations, based on observations on three related cases.** *Acta Neurochir* 1995;137:38–43
13. Kaar GF, N'Dow JM, Bashir SH. **Cervical spondylotic myelopathy with syringomyelia.** *Br J Neurosurg* 1996;10:413–415
14. Aubin ML, Baleriaux D, Cosnard G, et al. **MRI in syringomyelia of congenital, infectious, traumatic or idiopathic origin: a study of 142 cases.** *J Neuroradiol* 1987;4:313–336
15. Houang MT, Stern M, Brew B, Pell M, Darveniza P. **Magnetic resonance imaging (MRI) appearances of syringohydromyelia.** *Australas Radiol* 1988;32:172–177
16. Williams B, Bentley J. **Experimental communicating syringomyelia in dogs after cisternal kaolin injection, I: morphology.** *J Neurol Sci* 1980;48:93–107
17. Cho KH, Iwasaki Y, Imamura H, Hida K, Abe H. **Experimental model of posttraumatic syringomyelia: the role of adhesive arachnoiditis in syrinx formation.** *J Neurosurg* 1994;80:133–139
18. Milhorat TH, Nobandegani F, Miller JI, Rao C. **Noncommunicating syringomyelia following occlusion of central canal in rats.** *J Neurosurg* 1993;78:274–279
19. Oldfield EH, Muraszko K, Shawker TH, Patronas NJ. **Pathophysiology of syringomyelia associated with Chiari I malformation of the cerebellar tonsils.** *J Neurosurg* 1994;80:3–15
20. Rennels ML, Gregory TF, Blaumanis OR, Fujimoto K, Grady PA. **Evidence for a "paravascular" fluid circulation in the mammalian central nervous system, provided by the rapid distribution of tracer protein throughout the brain from the subarachnoid space.** *Brain Res* 1985;326:47–63
21. Rennels ML, Blaumanis OR, Grady PA. **Rapid solute transport throughout the brain via paravascular fluid pathways.** *Adv Neurol* 1990;52:431–439
22. Stoodley MA, Jones NR, Brown CJ. **Evidence for rapid fluid flow from the subarachnoid space into the spinal cord central canal in the rat.** *Brain Res* 1996;707:155–164
23. Stoodley MA, Brown SA, Brown CJ, Jones NR. **Arterial pulsation-dependent perivascular cerebrospinal fluid flow into the central canal in the sheep spinal cord.** *J Neurosurg* 1997;86:686–693
24. Cifuentes M, Fernandez-Llebrez P, Perez J, Perez-Figares JM, Rodriguez EM. **Distribution of intraventricularly injected horseradish peroxidase in cerebrospinal fluid compartments of the rat spinal cord.** *Cell Tissue Res* 1992;270:485–494
25. Milhorat TH, Adler DE, Heger IM, Miller JI, Hollenberg-Sher JR. **Histopathology of experimental hematomyelia.** *J Neurosurg* 1991; 75:911–915
26. Milhorat TH, Miller JI, Johnson WD, Adler DE, Heger IM. **Anatomical basis of syringomyelia occurring with hindbrain lesions.** *Neurosurgery* 1993;32:748–754
27. Milhorat TH, Johnson WD, Miller JI, Bergland RM, Hollenberg-Sher J. **Surgical treatment of syringomyelia based on magnetic resonance imaging criteria.** *Neurosurgery* 1992;31:231–245
28. Milhorat TH, Johnson RW, Milhorat RH, Capocelli AL, Pevsner PH. **Clinicopathological correlations in syringomyelia using axial magnetic resonance imaging.** *Neurosurgery* 1995;37:206–213
29. Milhorat TH, Kotzen RM, Anzil AP. **Stenosis of central canal of spinal cord in man: incidence and pathological findings in 232 autopsy cases.** *J Neurosurg* 1994;80:716–722
30. Lee TT, Arias JM, Andrus HL, Quencer RM, Falcone SF, Green BA. **Progressive posttraumatic myelomalacic myelopathy: treatment with untethering and expansive duraplasty.** *J Neurosurg* 1997;86:624–628
31. Falcone S, Quencer RM, Green B, Patchen SJ, Post MJD. **Progressive posttraumatic myelomalacic myelopathy: imaging and clinical features.** *AJNR Am J Neuroradiol* 1994;15:747–754
32. MacDonald RL, Findlay JM, Tator CH. **Microcystic spinal cord degeneration causing posttraumatic myelopathy: report of two cases.** *J Neurosurg* 1988;68:466–471
33. Osborne DRS, Vavoulis G, Nashold BS, Dubois PJ, Drayer BP, Heinz RE. **Late sequelae of spinal cord trauma: myelographic and surgical correlation.** *J Neurosurg* 1982;57:18–23
34. Gebarski SS, Maynard FW, Gabrielsen TO, Knake JE, Latack JT, Hoff JT. **Posttraumatic progressive myelopathy.** *Radiology* 1985;157:379–385
35. Stevens JM, Olney JS, Kendall BE. **Post-traumatic cystic and non-cystic myelopathy.** *Neuroradiology* 1985;27:48–56
36. Tanghe HLJ. **Magnetic resonance imaging (MRI) in syringomyelia.** *Acta Neurochir* 1995;134:93–99
37. Quencer RM, Morse BMM, Green BA, Eismont FJ, Brost P. **Intraoperative spinal sonography: adjunct to metrizamide CT in the assessment and surgical decompression of posttraumatic spinal cord cysts.** *AJR Am J Roentgenol* 1984;142:593–601
38. Wilberger JE Jr, Maroon JC, Prostko ER, Baghai P, Beckman I, Deeb Z. **Magnetic resonance imaging and intraoperative neurosonography in syringomyelia.** *Neurosurgery* 1987;20:599–605
39. Jinkins JR, Reddy S, Leite CC, Bazan C, Xiong L. **MR of parenchymal spinal cord signal change as a sign of active advancement in clinically progressive posttraumatic syringomyelia.** *AJNR Am J Neuroradiol* 1998;19:177–182
40. Morioka T, Shono T, Nishio S, Yoshida K, Hasuo K, Fukui M. **Acquired Chiari I malformation and syringomyelia associated with bilateral chronic subdural hematoma: case report.** *J Neurosurg* 1995;83:556–558
41. Schievink WI, Atkinson JLD. **Spontaneous intracranial hypotension (letter).** *J Neurosurg* 1996;84:151–152
42. Mamelak AN, Fishman RA, Dillon WP, Wilson CB. **Spontaneous intracranial hypotension (letter).** *J Neurosurg* 1996;85:192–193
43. Tator CH, Koyanagi I. Vascular mechanisms in the pathophysiology of human spinal cord injury. *J Neurosurg* 1997;86:483–492
44. Watson N. **Ascending cystic degeneration of the cord after spinal cord injury.** *Paraplegia* 1981;19:89–95
45. Hutchings M, Weller RO. **Anatomical relationships of the pia mater to cerebral blood vessels in man.** *J Neurosurg* 1986;65: 316–325
46. Zhang ET, Inman CBE, Weller RO. **Interrelationships of the pia mater and the perivascular (Virchow-Robin) spaces in the human cerebrum.** *J Anat* 1990;170:111–123